

Isothermal Crystallization Behavior of Metallocene-catalyzed Isotactic Polypropylene

Deukkil Park,¹ Il Kim,¹ Yang-Kyu Han,² Soo-Deuk Seul,³ Bu-Ung Kim,⁴ Chang-Sik Ha¹

¹Department of Polymer Science and Engineering, Pusan National University, Pusan 609–735, Korea

²Department of Chemistry, Hanyang University, Seoul 133–791, Korea

³Department of Chemical Engineering, Dong-A University, Pusan 602–711, Korea

⁴Department of Chemical Engineering, Pusan National University, Pusan 609–735, Korea

Received 29 December 2003; accepted 1 August 2004

DOI 10.1002/app.21253

Published online in Wiley InterScience (www.interscience.wiley.com).

ABSTRACT: Isothermal crystallization behavior of isotactic polypropylene (iPP) synthesized using metallocene catalyst was investigated in this work. The isotacticity of the polypropylene was characterized by ¹³C-NMR spectroscopy. It was found that the melting temperature (T_m) of the iPP is 123.51°C and the crystallization temperature (T_c) is 93°C. The iPP synthesized in this work did not show a general increase of T_m with an increase of crystallization temperature T_c , due to the short crystallization time of 20 min and low molecular weight (number average molecular weight = 6,300). The iPP showed a tendency of increasing heat of fusion (ΔH_f) with decreasing crystallization temper-

ature. All the spherulites of iPP samples showed negative birefringence. For the iPP sample crystallized at the highest T_c (= 123°C, just below T_m), the spherulite showed a pronounced Maltese Cross and a continuous sheaf-like texture aligning radially, which suggests that *R*-lamellae are dominant in this spherulite. The crystalline structure of the iPP was also investigated by X-ray diffraction. © 2004 Wiley Periodicals, Inc. *J Appl Polym Sci* 95: 231–237, 2005

Key words: isotactic; polypropylene; metallocene catalysts; crystallization

INTRODUCTION

One of the main advances in the polyolefin technology in the last decade was the use of single-site metallocene catalysts to produce a new variety of ethylene and α -olefinic copolymers.¹ It enables polyolefinic materials to strengthen their presence in the fields of elastomers and plastomers. These catalysts permit improved control of molecular weight (M_w), molecular weight distribution (MWD), and short-chain branching (SCB), which can be used to enhance the performance of the final product. Due to the uniformity of the polypropylene (PP) chains, for instance, metallocene-catalyzed PP has a very narrow weight distribution (M_w/M_n of 2–3) compared to conventional PP (minimum M_w/M_n of 3–6).

Even if the occurrence of the set of transverse crystallites for the metallocene-catalyzed PP is known, it still remains a difficult matter to analyze the crystallization and melting processes for a given sample.² In this sense, crystallization and melting characteristics of the metallocene-catalyzed iPP have recently attracted interest from both theoretical and practical points of view.^{3–7} Most of the previous works reported

until now, however, dealt with crystallization and melting behaviors of metallocene-catalyzed PP with high molecular weight [usually number average molecular weight (M_n) > ~ 100,000] and thus crystallization behaviors at high crystallization temperatures (> 95 ~ 135°C).

PP can exist in different morphological forms, depending on the tacticity and the crystallization conditions, such as pressure, temperature, and cooling rate.⁸ Different forms can coexist, and one polymorphic form can change into another as conditions change. Furthermore, the crystallization and melting behaviors of PP strongly depend on its inherent physicochemical characteristics, such as the molecular weight and the molecular weight distribution. In the present work, we report the spherulitic morphology of melt-crystallized thin film samples of the PP of low molecular weight (M_n of ~ 7000) synthesized using a metallocene catalyst, depending on the crystallization temperature.

EXPERIMENTAL

Polymerization

Propylene (99.5%, polymer grade, Matheson) was purified by passage through a Matheson 6410 gas purification column. Toluene was distilled from sodium under nitrogen. The metallocene catalyst compound,

Correspondence to: C.-S. Ha (csaha@pusan.ac.kr).

rac-(EBI)Zr-(NMe₂)₂, was synthesized by procedures described in the literature.⁹ Methylaluminoxane (MAO) was donated by Albemarle as a 10% solution in toluene, which contained 1.85 wt % MAO (4.49 wt % total Al). AlMe₃ and Al(iBu)₃ were obtained from Aldrich and used without further purification. [Ph₃C][B(C₆F₅)₄] was donated by Asahi Glass Co., Ltd. Propylene polymerization was performed in a 250-mL Fisher-Porter reactor equipped with a mechanical stirrer and a temperature probe. In a drybox the reactor was charged with toluene (120 mL), and the prescribed amount of alkyl aluminum reagent was added. The metallocene compound (2.5 mg) was then added. After the metallocene catalyst was dissolved, the activator [Ph₃C][B(C₆F₅)₄] was added. The reactor was immersed in a constant temperature bath previously set to the desired temperature, and the stirrer was turned on. When the reactor temperature had equilibrated to the bath temperature, polymerization was initiated by pressurizing the reactor with propylene (1 atm). The pressure was maintained at 1 atm.

Polymerization was quenched by addition of EtOH (~ 200 mL) followed by concentrated HCl (20 mL). The PP was isolated by filtration, washed several times with EtOH, and dried (70°C, vacuum oven, overnight).

Measurements

The molecular weight (M_w) was evaluated by a gel permeation chromatography (GPC). Analyzes were undertaken using 1,2,4-trichlorobenzene as solvent at 135°C and $M_{w,s}$ were calculated using a universal calibration curve built with polyethylene, PP, and polystyrene standards (American Polymer Standard Corp.). Molecular weight of the PP in this work as determined by GPC (Waters 150-C) was 11,900 and its molecular weight distribution (M_w/M_n) was 1.9.

The tacticity of the PP synthesized in this work was measured by ¹³C-NMR spectroscopy on a Varian Unity Plus 300 Spectrometer operating at 75.45 MHz. The polymer was dissolved in 1,2,4-trichlorobenzene (5% wt/vol) and observed at 120°C (393.1 K) with broad band and proton decoupling and 60.2° pulse. In this work, the average tacticity was precisely characterized by the content of *meso*-pentads (*mmmm*%) determined from the methyl carbon resonance data. From a practical point of view, the content of *mmmm* pentad sequences is calculated using methyl peaks resonating between 19 and 22 ppm following the relationship:

$$mmmm\% = (S_{mmmm}/S_{\text{total methyl}}) \times 100$$

ASi ReactIRTM 1000 was also used to evaluate the isotacticity of the polypropylene synthesized in this work.

A thermal analyses TA 100 calorimeter was used to determine melting temperatures. Discs cut out from films were heated in closed pans from room temperature to 180°C, held at this temperature for 5 min, cooled down to -50°C, and then heated again to 180°C. The heating and cooling rates were 10°C/min. The analyses were performed under nitrogen flux. Melting temperatures and degree of crystallinity were determined in the second scan.

A LEICA DMRXP microscope with polarized light equipped with a hot stage was used to study the morphology and crystallization of the PP. Images were captured using a Hitachi KP C550 CCD color camera. The samples were placed between glass slides and cover slips in a hot stage to 200°C for 5 min prior to rapid cooling to the isothermal crystallization temperature. The isothermal crystallization temperatures were selected to be 60, 70, 80, 93, and 123°C. After a time long enough for PP to crystallize completely (approximately 20 min) at a given crystallization temperature, the glass slides were taken out of the hot stage and were quenched in ice water for further X-ray diffraction measurements.

Wide angle X-ray diffraction patterns were obtained with Nickel-filtered CuK α radiation at 30 kV and 15 mA. The diffraction patterns of the isothermally crystallized PP samples as well as the as-prepared PP powder samples were performed with a Rigaku Miniflex diffractometer.

RESULTS AND DISCUSSION

A C²-symmetric metallocene with a Si-atom bridging the two ligands, due to higher stereoridity and favorable electronic characteristics, affords iPP with higher molecular weight and isotacticity.¹⁰ ¹³C-NMR analysis was used to characterize the average tacticity in terms of the overall content of *meso* (*m*) or racemic (*r*) configuration for a given fraction.¹¹ The main head-to-tail methyl resonances are shown in Figure 1 with all pentads stereosequence assignments. The strong resonances of methylene, methine, and methyl carbons of PP are observed at about 46, 28, and 21 ppm. The resonance peaks resulting from regio defects (2,1 erythro and 1,3 misinsertions) and chain ends (isobutyl, *n*-propyl, and vinyl) are properly assigned according to the literature.¹² The *meso* pentad content is 82.5%, with a significant deviation from simple Bernoullian statistics. The conventional interpretation of this analysis is that the polymer appears to be stereoblock, with predominantly isotactic sequences and a smaller fraction of syndiotactic sequences. The structure of the isotactic PP (iPP) was also confirmed in the IR spectrum, especially in the 800–1,200 cm⁻¹ range.² These bands are attributed to the 3_1 helix, which is the regular conformation in all iPP polymorphs, as well as in the mesomorphic phase. As shown in Figure 2, two

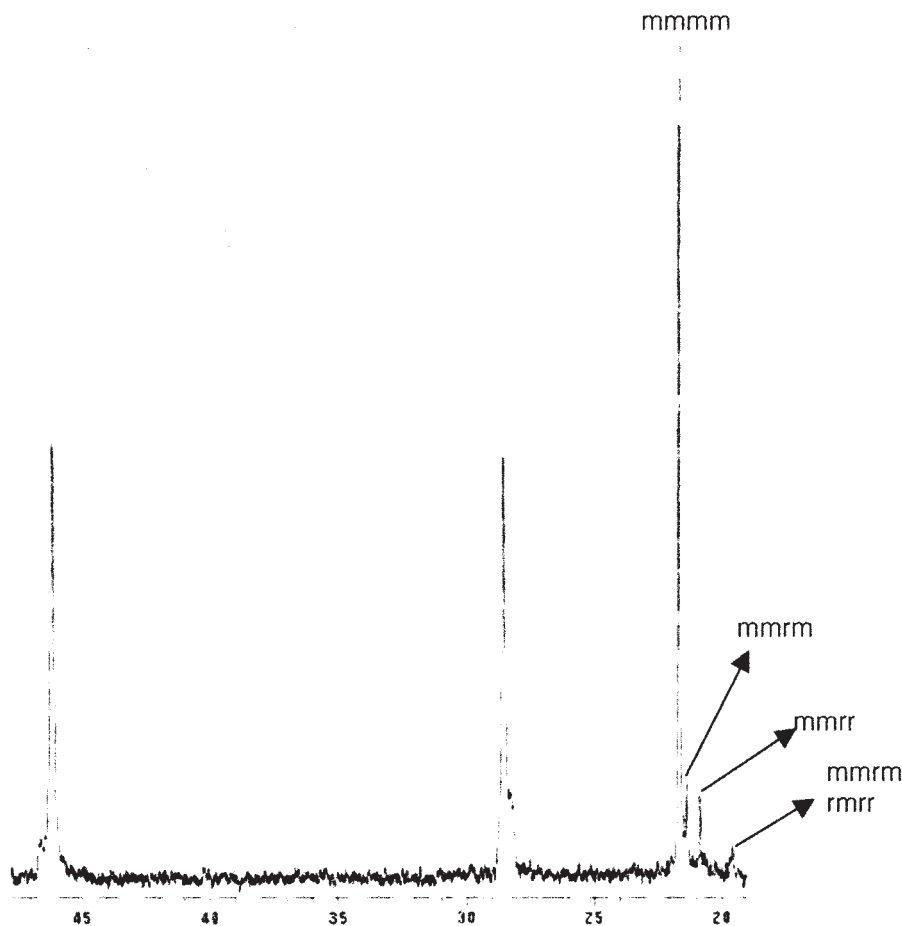


Figure 1 Expansion of the 75.45 MHz methyl carbon-13 NMR signal of the PP prepared with a metallocene catalyst in this work, which clearly shows the main isotactic peak.

commonly used “helix bands,” at 998 and 841 cm^{-1} , only appear for helix segments with at least ~ 11 and ~ 14 repeat units, respectively. The band at 973 cm^{-1}

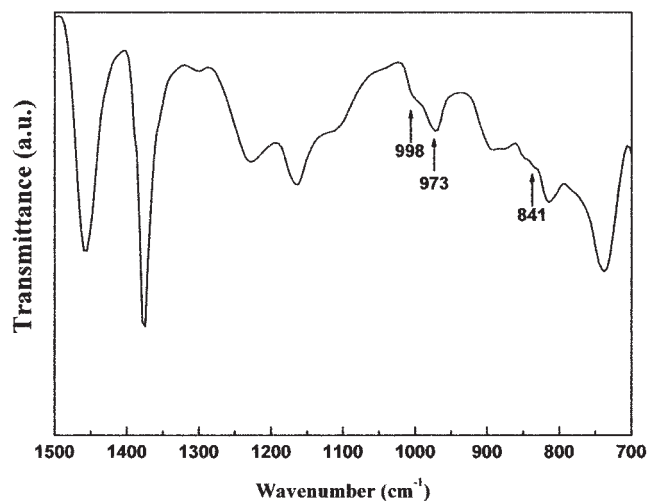


Figure 2 FTIR spectrum of the metallocene-catalyzed iPP in the wavenumber range of 700–1,500 cm^{-1} .

is attributed to shorter helix segments. Because the ability to form regular helices depends on the degree of isotacticity, the latter can be estimated indirectly using the helix bands.

Typical melting behavior observed by DSC for the metallocene-catalyzed iPP is shown in Figure 3. It was observed that the melting temperature (T_m) is 123.51°C and the crystallization temperature (T_c) is 93°C. The comparatively low T_m of the PP produced in this study despite the high stereospecificity seems to be related to the misinsertion of the monomer as already reported in our previous work⁹ and by Roll et al.¹² We checked 1,3-misinsertions, which arise from a tail-to-tail (2,1) insertion of the propylene monomer into the metal-polymer bond and the subsequent isomerization of the ensuing species with a secondary alkyl ligand, of the representative polymers that show extremely high $[m m m m]$ value.¹² The iPP of the present study was characterized by a low frequency of misinsertion (0.51%). However, the misinsertion amount seems to be enough to lower the T_m of the polymer.⁹ The lower T_m is also caused by the low molecular weight (ca. $M_n = 6300$) of the iPP, which is

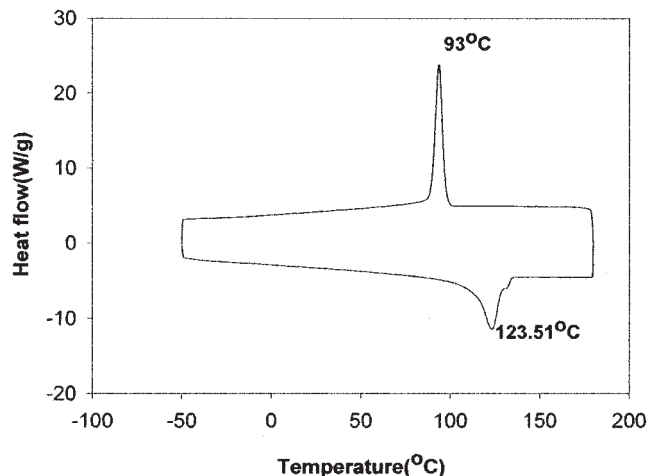


Figure 3 DSC thermogram of the metallocene-catalyzed iPP.

usually caused by performing the polymerization at a low monomer concentration.

The characterization of iPP crystallization at a given temperature for 20 min from DSC thermograms shown in Figure 4 is summarized in Table I. The crystallinity (X_c) of PP was calculated from the heat of fusion ratio, $(\Delta H_f/\Delta H_{f0}) \times 100$, in which ΔH_f is the heat of fusion of the sample as determined from the DSC curve, and ΔH_{f0} is the fusion of folded chain of iPP with the value of 208.3 J/g^4 . Maiti et al.¹³ showed systematic increase of melting temperature T_m with the increase of the crystallization temperature T_c and the crystallization time t at $T_c = 160^\circ\text{C}$, respectively. It is seen that the change of T_m versus T_c is much more evident than that of T_m versus t at a constant T_c . As a matter of fact, T_m increases linearly with logarithmic crystallization time, $\log t$. However, the iPP used in

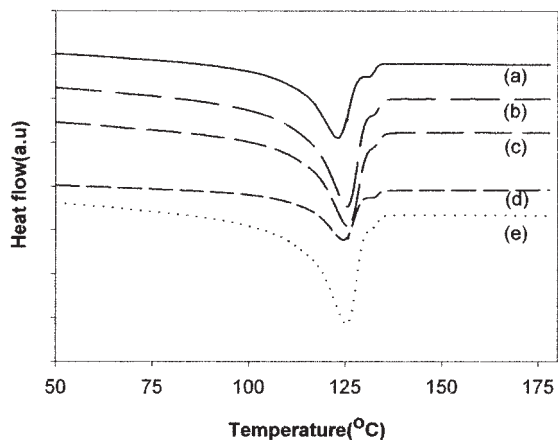


Figure 4 Heat flow versus temperature during isothermal crystallization at a given temperature for 20 min: (a) $T_c = 123^\circ\text{C}$; (b) $T_c = 93^\circ\text{C}$; (c) $T_c = 80^\circ\text{C}$; (d) $T_c = 70^\circ\text{C}$; and (e) $T_c = 60^\circ\text{C}$.

TABLE I
Characterization of the Metallocene-catalyzed iPP
Crystallized at a Given Temperature for 20 min
Using DSC Thermograms

Crystallization temperature ($^\circ\text{C}$)	T_m ($^\circ\text{C}$)	T_c ($^\circ\text{C}$)	ΔH (J/g)	Crystallinity (X_c , %)
60	125.1	95.6	119.4	58
70	124.6	95.5	114.2	55
80	125.7	94.2	105.0	51
93	125.3	95.5	106.0	51
123	123.0	94.8	94.7	46
iPP powder	123.5	93.5	77.1	37

this work did not show a general increase of T_m with an increase in the crystallization temperature T_c . This is due to the short crystallization time (i.e., for 20 min) in comparison to the work of Maiti et al.,¹³ in which they used crystallization times from 48 h to 180 days.

As a first approximation, the isothermal crystallization can be determined by the Avrami equation as follows:^{14,15}

$$I - X_{ti} = \exp(-Kt)^n \quad (1)$$

where X_{ti} is the relative crystallinity at crystallization time t , K is a crystallization kinetic constant, and n is the Avrami exponent. The equation tells us that, upon increasing the crystallization time, the crystallinity at a given crystallization time increases in a sigmoidal mode. Therefore, there is not much change in the crystallinity both at the initial time of crystallization (i.e., short crystallization time) as well as the final crystallization time (i.e., at the last stage of crystallization). Thus, T_m will not be much different from T_c at the initial crystallization time. It is well known that the crystallization rate becomes nucleation-controlled at high temperatures and growth-controlled at low temperatures, meaning a low crystallization rate at a low crystallization temperature.

Furthermore, T_m can be expressed by the following modified Hoffamn equation [eq. (2)].³

$$T_m = T_m^0 \left(1 - \frac{2\sigma_e}{\Delta h_f \beta l} \right) \quad (2)$$

where T_m^0 is the equilibrium melting temperature, σ_e is the surface free energy of fold plane of lamella, Δh_f is the heat of fusion, and l is the thickness of lamella. It was suggested that the T_m is not related with crystals with mean lamellar thickness l but with crystals with a step height βl . The β is determined by the distribution of l .³

Since the metallocene-catalyzed iPP is polymerized by a single-site catalyst, its intermolecular distribution of defects (stereoirregular and reioirregular bonds) is generally uniform. Accordingly, at the time of crystal-

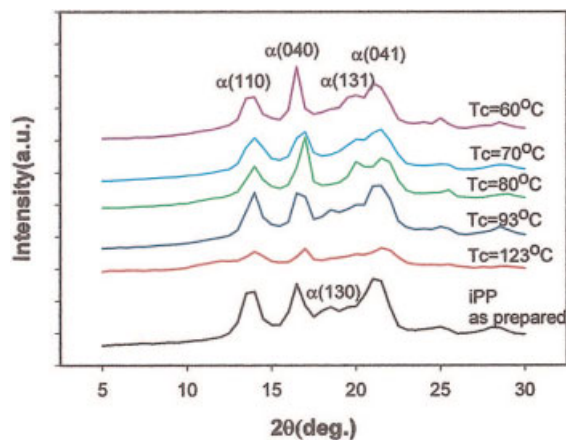


Figure 5 XRD patterns with assigned reflections of the metalocene-catalyzed iPP obtained after completion of isothermal crystallization at indicated temperatures (θ ; Bragg diffraction angle).

lization, the defects are rejected from or incorporated in lamellar crystals, which results in thinning of the lamellae or in disordering of crystalline quality. The uniform distributions of stereoirregular bonds and copolymerization bonds will also make the distribution of crystallinity (isotactic sequence length) narrow.³ The thickness of lamellae of the metalocene-catalyzed iPP is then not only thin but also uniform, and hence β in eq. (2) is low, which is assumed to lead a low observed T_m .

Therefore, it may be not surprising that, in this work, the T_m of the metalocene-catalyzed iPP remains nearly unchanged despite the increase in T_c due to the combined effects of short crystallization times (~ 20 min) and lower crystallization temperature (i.e., the maximum crystallization temperature; $\sim 93^\circ\text{C}$). The unusual crystallization and melting behaviors of the present metalocene-catalyzed iPP are also related to the low molecular weight. As one can see in Table I, however, the metalocene-catalyzed iPP shows an increasing tendency of ΔH_f with decreasing crystallization temperature, as is generally expected. It may be considered that the crystallization behavior at high crystallization temperatures ($> 95 \sim 123^\circ\text{C}$) is similar as that of other metalocene-catalyzed iPP reported until now,³⁻⁷ though more details on this subject will be reported elsewhere.

Figure 5 shows WAXD patterns measured at different crystallization temperatures (T_c s) for 20 min. The analysis of the relative intensities of the X-ray diffraction from all the samples are based on the diffraction pattern of the iPP as prepared. In Figure 5, four sharp crystalline reflection peaks, in the region of the Bragg angle (2θ) between 10 and 30° are observed. Those strong diffraction peaks are located at the diffraction angles 2θ of 14.0 , 17.0 , 21.7 , and 23.2° . They have been labeled with the indices (110), (040), (131), and (041),

respectively.¹⁶ A weak crystalline reflection peak, in the region of the 2θ of 18.5° labeled with (130), is shown for the iPP as prepared only. This peak disappeared for the other five samples measured after crystallization for 20 min. It is seen from this diffractogram that the iPP sample used in this study has the α -form or monoclinic structure.¹⁷ However, a remarkable crystallographic transformation is evidenced during crystallizing from 93 to 60°C . The intensity of a peak at $2\theta = 21.7^\circ$ is seen to be increased, while at the same time the other reflections are being narrowed. Four types of spherulites are observed to grow from the melt in iPP according to Padden and Keith.¹⁸ They explained that type I spherulites exhibited positive birefringence in the radial direction and a simple Maltese Cross with a coarse branching radial structure due to the preferred crystalline orientation in the amorphous areas brought about by radial contraction during crystallization at high degree of supercooling. They further reported for X-ray diffraction studies of PP¹⁹ that the most commonly occurring types of spherulites (type I and type II) can be identified as the monoclinic structure whereas type III and type IV spherulites to exhibit negative birefringence are categorized in the second metastable β -crystalline forms.

The thermal conditions (crystallization temperature, cooling rate) of crystallization govern not only the type and optical character of spherulites, the polymorphic composition and the thermophysical characteristics (e.g., T_m) of the samples obtained, but also influence the size and size distribution of the spherulites.²⁰ By reducing the crystallization temperature or by increasing the cooling rate, the average spherulite size decreases due to an increase in the average density of nuclei. With increasing temperature, the spherulitic texture becomes relatively coarse with irregular Maltese Cross extinction.²¹

Optical micrographs of the metalocene-catalyzed iPP spherulites are shown in Figure 6. All of the spherulites of the iPP samples showed negative birefringence. For the iPP sample crystallized at the highest T_c ($= 123^\circ\text{C}$, just below the T_m of the iPP), the spherulite shows a pronounced Maltese Cross and a continuous sheaf-like texture aligning radially, which suggests that R -lamellae (crosshatching within a spherulite is composed of radial lamellae) are dominant in this spherulite.¹³ It should be noted, however, that the occurrence of spontaneous crystallization will make the Maltese Cross difficult to observe when T_c is lower (93°C in this work), as expected.

CONCLUSION

In this work, isotactic polypropylene was synthesized using a metalocene catalyst. The molecular weight of the iPP was determined as $11,900$ g/mol by GPC and M_w/M_n was 1.9. The synthesized iPP was character-

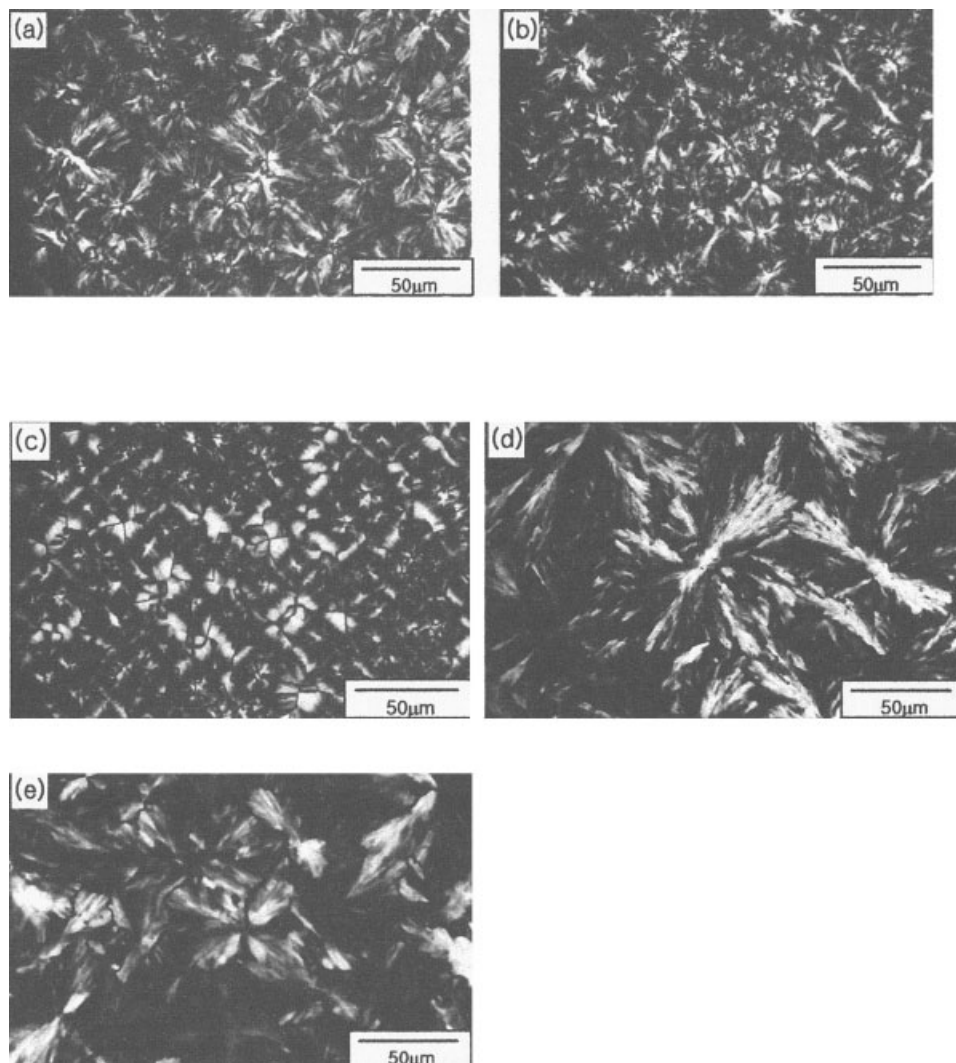


Figure 6 Typical spherulitic morphology of the metallocene-catalyzed iPP crystallized at different temperatures for 20 min observed by polarizing optical microscopy: (a) 123°C, (b) 93°C, (c) 80°C, (d) 70°C, and (e) 60°C.

ized by ^{13}C -NMR spectroscopy, which shows high isotacticity (87.5%). It was found that the melting temperature (T_m) of the iPP was 123.51°C and the crystallization temperature (T_c) was 93°C. The comparatively low T_m of the iPP despite their high stereospecificity was reported presumably to be related with the misinsertion of the monomer. The iPP did not show a general increase of T_m with increasing of crystallization temperature T_c , due to the short crystallization time of 20 min and low molecular weight. However, the iPP showed an increasing tendency in the heat of fusion (ΔH_f) with decreasing crystallization temperature. The XRD pattern of the iPP synthesized in this work showed the α -form crystalline structure. All of the spherulites of the iPP samples crystallized at different temperatures, ranging from 63 to 123°C, showed negative birefringence. For the iPP sample crystallized at the highest T_c (= 123°C, just below T_m), the spherulite showed a pronounced Maltese Cross

and a continuous sheaf-like texture aligning radially, which suggests that *R*-lamellae are dominant in this spherulite.

The work was financially supported by the National Research Laboratory Program, the Center for Integrated Molecular Systems (CSHa), the Center for Ultramicrochemical Process Systems (IKim), the Center for Advanced Net Shape Manufacturing and Clean Processes (SDSeul), and the Brain Korea 21 Project.

References

1. Wood-Adams, P. M.; Dealy, J. M.; deGroot, A. W.; Redwine, A. D. *Macromolecules* 2000, 33, 7489.
2. Karger-Kocsis, J. In *Polypropylene: An A-Z Reference*; Kluwer Publishers: Dordrecht, 1999.
3. Fujiyama, M.; Inata, H. *J Appl Polym Sci* 2002, 85, 1851.
4. Bond, E. B.; Spruiell, J. H.; Lin, J. S. *J Polym Sci Polym Phys* 1999, 37, 3050.

5. Dai, P. S.; Cebe, P.; Capel, M. *J Polym Sci Polym Phys* 2002, 40, 1644.
6. Xu, J. T.; Guan, F. X.; Yasin, T.; Fan, Z. Q. *J Appl Polym Sci* 2003, 90, 3215.
7. Gahleitner, M.; Bachner, C.; Ratajski, E.; Rohaczek, G.; Neissl, W. *J Appl Polym Sci* 1999, 73, 2507.
8. Maier, C.; Calafut, T. In *Polypropylene: Plastics Design Library*; Academic Press: New York, 1998, pp 10–15.
9. Kim, I.; Zhou, J. M.; Won, M. S.; *J Polym Sci Polym Chem* 1999, 37, 737.
10. Viville, P.; Daoust, D.; Jonas, A. M.; Dupire, M.; Debras, G. *Polymer* 1953, 2001, 42.
11. Zambelli, A.; Locatelli, P.; Provasoli, A.; Ferro, D. R. *Macromolecules* 1980, 13, 267.
12. Roll, W.; Brintzinger, H. H.; Rieger, B.; Zolk, R. *Angew Chem Int Ed Engl* 1990, 29, 279.
13. Maiti, P.; Hikosaka, M.; Yamada, K.; Toda, A.; Gu, F. *Macromolecules* 2000, 33, 9069.
14. Jang, G. S.; Cho, W. J.; Ha, C. S. *J Polym Sci Polym Phys* 2001, 39, 1001.
15. Ha, C. S.; Cho, Y. W.; Cho, W. J.; Kim, Y.; Inoue, T. *Polym Eng Sci* 2000, 40, 1816.
16. Ha, C. S.; Kim, S. C. *J Appl Polym Sci* 1988, 35, 2211.
17. Vieweg, R.; Schley, A.; Schwarz, I. A. In *Polyolefine: Kunststoffhandbuch IV*; Hanser Verlag: Munchen, 1969, pp 33–42.
18. Padden, F. J.; Keith, H. D. *J Appl Phys* 1959, 30, 1479.
19. Keith H. D.; Padden, F. J.; Walter, N. M.; Wycoff, M. W. *J Appl Phys* 1959, 30, 1485.
20. Varga, J. *J Mater Sci* 1992, 27, 2557.
21. Rodriguez-Arnold, J.; Bu, Z.; Cheng, S. Z. D.; Eric, T.; Hsieh, E. T.; Johnson, T. M.; Geerts, R. G.; Palackal, S. J.; Hawley, G. R.; Welch, M. B. *Polymer* 1994, 35, 5194.